JACS
JOURNAL OF THE AMERICAN CHEMICAL SOCIETY

Subscriber access provided by Kaohsiung Medical University

Article

Enantioselective Synthesis of des-epoxy-Amphidinolide N

Barry M. Trost, Wen-Ju Bai, Craig E. Stivala, Christoph Hohn, Caroline Poock, Marc Heinrich, Shiyan Xu, and Jullien Rey

J. Am. Chem. Soc., **Just Accepted Manuscript** • DOI: 10.1021/jacs.8b11827 • Publication Date (Web): 20 Nov 2018

Downloaded from http://pubs.acs.org on November 20, 2018

Just Accepted

"Just Accepted" manuscripts have been peer-reviewed and accepted for publication. They are posted online prior to technical editing, formatting for publication and author proofing. The American Chemical Society provides "Just Accepted" as a service to the research community to expedite the dissemination of scientific material as soon as possible after acceptance. "Just Accepted" manuscripts appear in full in PDF format accompanied by an HTML abstract. "Just Accepted" manuscripts have been fully peer reviewed, but should not be considered the official version of record. They are citable by the Digital Object Identifier (DOI®). "Just Accepted" is an optional service offered to authors. Therefore, the "Just Accepted" Web site may not include all articles that will be published in the journal. After a manuscript is technically edited and formatted, it will be removed from the "Just Accepted" Web site and published as an ASAP article. Note that technical editing may introduce minor changes to the manuscript text and/or graphics which could affect content, and all legal disclaimers and ethical guidelines that apply to the journal pertain. ACS cannot be held responsible for errors or consequences arising from the use of information contained in these "Just Accepted" manuscripts.

ACS Publications

is published by the American Chemical Society. 1155 Sixteenth Street N.W., Washington, DC 20036

Published by American Chemical Society. Copyright © American Chemical Society. However, no copyright claim is made to original U.S. Government works, or works produced by employees of any Commonwealth realm Crown government in the course of their duties.

Enantioselective Synthesis of *des*-epoxy-Amphidinolide N

Barry M. Trost,* Wen-Ju Bai, Craig E. Stivala, Christoph Hohn, Caroline Poock, Marc Heinrich, Shiyan Xu, Julien Rey

Department of Chemistry, Stanford University, Stanford, California 94305-5080, United States

ABSTRACT: The synthesis of *des*-epoxy-amphidinolide N was achieved in 22 longest linear and 33 total steps. Three generations of synthetic endeavors are reported herein. During the first generation, our key stitching strategy that highlighted an intramolecular Ru-catalyzed alkene-alkyne (Ru AA) coupling and a late-stage epoxidation proved successful, but the installation of the α,α'-dihydroxyl ketone motif employing a dihydroxylation method was problematic. Our second generation of synthetic efforts addressed the scalability problem of the southern fragment synthesis and significantly improved the efficiency of the atom-economical Ru AA coupling, but suffered from several protecting group-based issues that proved insurmountable. Finally, relying on a judicious protecting group strategy together with concise fragment preparation, *des*-epoxy-amphidinolide N was achieved in a convergent fashion. Calculations disclose a hydrogen-bonding bridge within amphidinolide N. Comparisons of ^{13}C NMR chemical shift differences using our synthetic *des*-epoxy-amphidinolide N suggest that amphidinolide N and carbenolide I are probably identical.

INTRODUCTION

Macrolides provide a remarkable source for drug development due to their marvelous structural diversity and biological activity. For example, everolimus, an anti-rejection drug that is listed as one of the *Top 100 Brand Name Drugs by Retail Sales in 2016*, is essentially a rapamycin derivative. Therefore, syntheses and biological assessments[1] of macrolides[2] and their analogues[3] have been enthusiastically pursued.

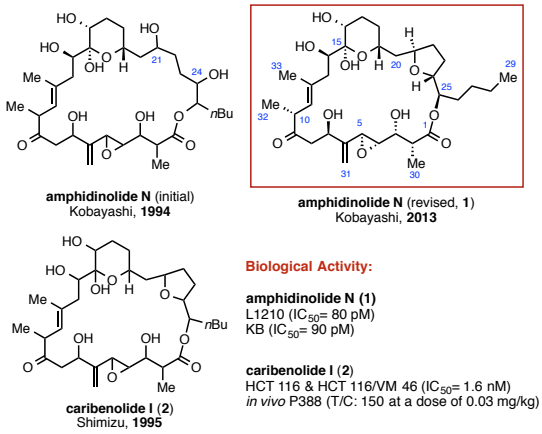

Figure 1. Structure and biological activity of amphidinolide N (**1**) and caribenolide I (**2**).

The amphidinolide family of natural products, isolated from the symbiotic dinoflagellates of the genus *Amphidinium* in Okinawa, is a unique class of cytotoxic macrolides.[4] Over 40 members have been disclosed by Kobayashi, among which amphidinolide N (**1**) exhibits the most potent cytotoxicity against murine lymphoma L1210 and human epidermoid carcinoma KB cell lines, with IC_{50} values of 80 and 90 pM, respectively (Figure 1).[5] Further evaluation of amphidinolide N as a potential chemotherapeutic agent has been impeded by a lack of material; the natural isolation yield (0.0009%) is meager, and biological efforts to improve product titers by modifying the culturing process have proven futile.[4a] The chemical structure of amphidinolide N was initially proposed to include two hydroxyl groups at C21 and C24 positions,[5a] which was revised two decades later as a THF ring along with stereochemical assignment relying on NMR studies.[5b] Within the amphidinolide family, similar tetrahydrofuran (THF) rings are common, such as in amphidinolide F.[6] However, a tetrahydropyran (THP) moiety is much scarcer, and a combination of THF and THP motifs has only been discovered in amphidinolide N (**1**), making it the most complicated family member with a total of 13 stereocenters. Consequently, amphidinolide N (**1**) has been an elusive target in spite of two decades of extensive synthetic studies.[7] Furthermore, synthesis of amphidinolide N (**1**) could also provide insight into the structure of caribenolide I (**2**), which was isolated from a free-swimming dinoflagellate of the genus *Amphidinium* in Caribbean Sea.[8] Harvested from different organisms on opposite hemispheres, amphidinolide N (**1**) and caribenolide I (**2**) possess comparable levels of cytotoxicity and identical connectivity, although the stereochemistry of the latter was never assigned. Previously, exploration of the structural relationship between amphidinolide N (**1**) and caribenolide I (**2**) was unrealistic, as their isolation spectra were recorded in C_6D_6 and CD_2Cl_2, respectively. Herein we report an enantioselective synthesis of *des*-epoxy-amphidinolide N (**41**) alongside our findings about the relationship between amphidinolide N (**1**) and caribenolide I (**2**).

RESULTS AND DISCUSSION

Retrosynthetically, amphidinolide N (**1**) was disconnected into two subunits **5** and **6** of similar size and structural complexity (Scheme 1). We expected to perform the C4-C5 epoxidation and the C15-hemiacetal formation on macrocycle **3** at a late stage. The intermediate **3** might arise from macrocyclic compound **4** by installing the desired α,α'-dihydroxy ketone motif alongside a C9-

OH oxidation. As the construction of the α,α'-dihydroxyl ketone moiety seemed challenging, we initially proposed two approaches, including a dihydroxylation method[9] and a Rubottom oxidation strategy.[10] The compound **4**, in turn, could be accessed by atom-economically[11] stitching fragments **5** and **6** together employing our Ru-catalyzed alkene-alkyne coupling[12] and an esterification.

Scheme 1. Initial Retrosynthetic Analysis

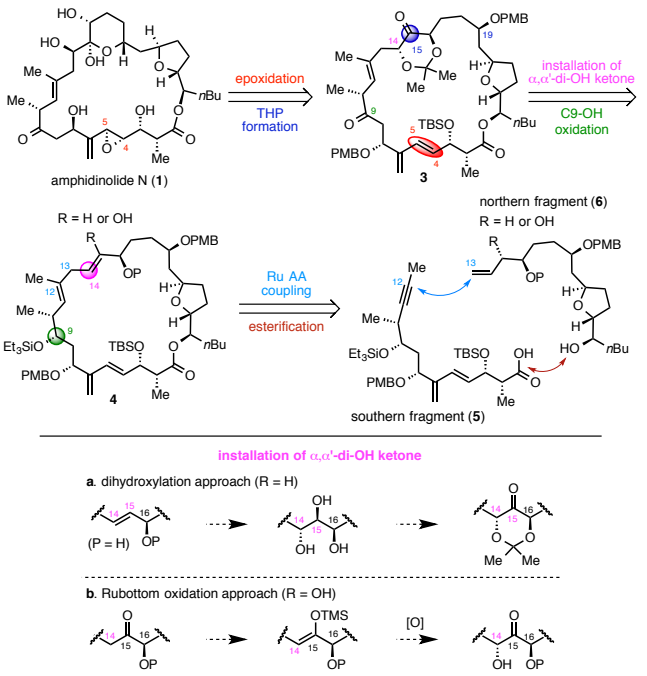

I. The First Generation of Synthetic Endeavors

The first generation of the southern fragment synthesis featured a Marshall coupling to install the propargyl group,[13] an enyne metathesis to create the diene,[14] and an Evans aldol[15] to generate the *syn* aldol-adduct (Scheme 2). The synthesis commenced with PMB protection of the known propargyl alcohol **7**, prepared in 4 steps from commercial materials via an enzymatic resolution.[16] Meanwhile, the known allylic alcohol **9** was accessed in 2 steps utilizing an Evans aldol reaction.[7a] The subsequent enyne metathesis was carefully investigated. While the typical conditions (10 mol% Grubbs-II, 10 mol% benzoquinone, DCE, 60°C)[17] provided diene **10** in meager yields ranging from 15-25%, addition of CuI

Scheme 2. Southern Fragment Synthesis (1st-Gen.)

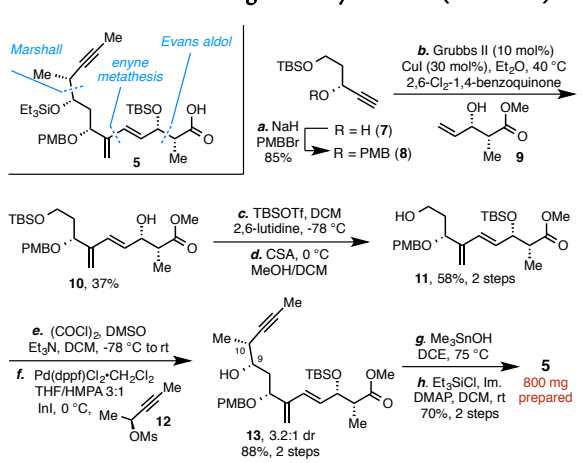

improved the yield to 33%.[18] Tuning the amounts of the CuI / benzoquinone additives slightly enhanced the yield to 37%, while further varying reaction concentration, temperature, or the reagent stoichiometry proved futile. Nevertheless, TBS protection of the metathesis product **10** followed by chemoselective protodesilylation of the primary TBS group using CSA in MeOH delivered alcohol **11**. A succeeding Moffatt-Swern oxidation[19] gave an aldehyde intermediate that was immediately subjected to Marshall coupling[13] with chiral propargyl mesylate **12**.[20] The stereochemistry of the newly generated C9-OH was confirmed by converting alcohol **13** to the corresponding mandelic esters,[21] while the C10 stereocenter was established by ROESY analysis of an intramolecular hydrosilylation product of alkyne **13**.[22] Treatment of the homopropargyl alcohol **13** with Me_3SnOH[23] followed by a triethylsilyl- (TES-) protection of the secondary alcohol provided 800 mg of the southern fragment **5** in 8 steps from known compound **7**.

Scheme 3. Northern Fragment Synthesis (1st-Gen.)

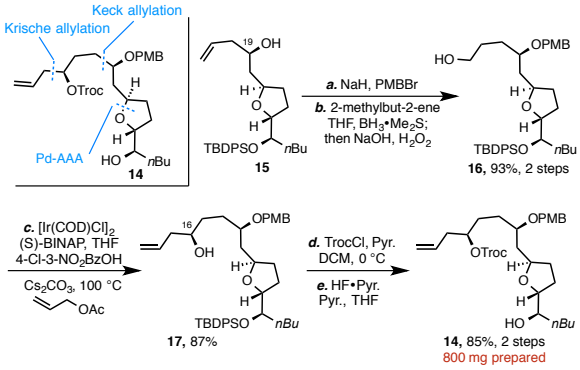

The northern fragment synthesis exploited a late-stage Krische allylation[24] to construct the homoallylic alcohol motif (Scheme 3). The starting alcohol **15** was prepared in 8 steps from commercially available materials,[7c] highlighting a Pd-asymmetric allylic alkylation (Pd-AAA) to build the *trans*-THF ring[25] and a Keck allylation[26] to extend the carbon chain. The C19-stereochemistry of alcohol **15** was confirmed by converting it to the corresponding mandelic esters.[21] Masking the known alcohol **15** as its PMB ether, followed by hydroboration/oxidation generated the primary alcohol **16**. The subsequent Ir-catalyzed allylation produced homoallylic alcohol **17** in excellent yield and diastereoselectivity.[24] The C16-OH stereochemistry of **17** was verified by converting the alcohol to the corresponding mandelic esters.[21] Troc-protection of alcohol **17** followed by removal of the TBDPS protecting group afforded 800 mg of the northern fragment **14**.

With both the southern and northern fragments in hand, we advanced the synthesis by testing our key stitching strategy: the Ru AA coupling and the esterification (Scheme 4). Ru AA coupling is known to generate both linear and branched products.[12] For example, linear selectivity was seen in an intermolecular Ru AA coupling during our synthesis of lasonolide A.[27] Unlike the prevalent intermolecular couplings, the intramolecular variant of this reaction is incredibly rare. To date, only three examples have been reported in the syntheses of amphidinolide A,[28] pinnatoxin A,[29] and laulimalide,[30] and branched selectivity was observed in all cases. Therefore, it seemed wise to first join the southern and northern fragments together using an intermolecular Ru AA coupling to obtain the linear selectivity, then perform an esterification to close the macrocyclic ring. However, preliminary results indicated that

Scheme 4. Assembly of the 1st-Generation of Southern and Northern Fragments

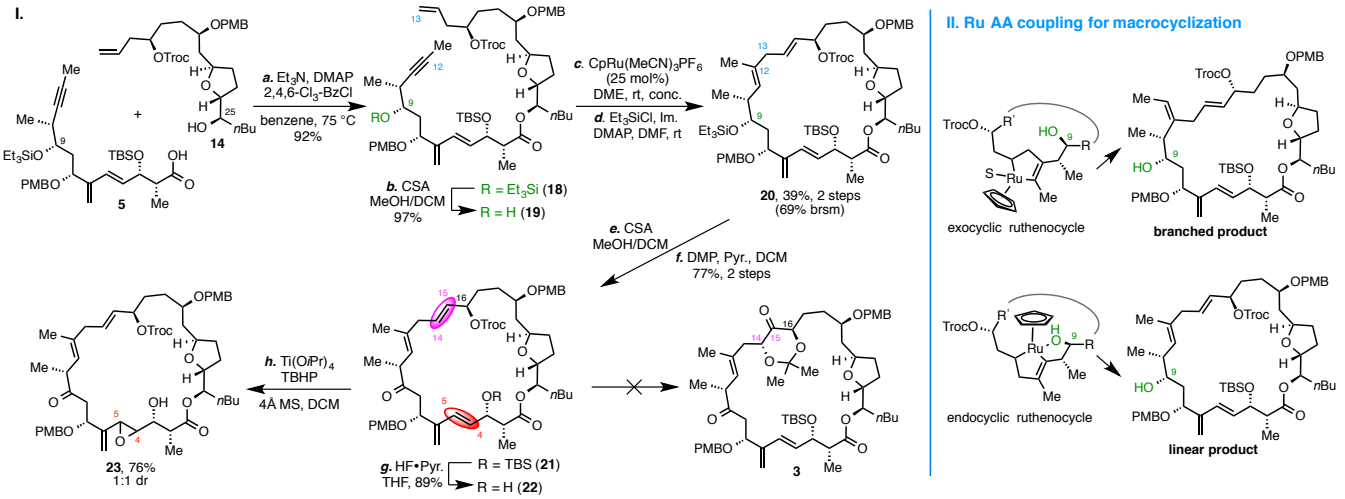

the C9-OTES needed to be unmasked to run the Ru AA coupling and unfortunately, the C9-OH instead of the C25-OH reacted in the following macrolactonization. As a result, we decided to reorder the sequence. Analysis of the ruthenacyclopentene intermediates for both the branched and linear products suggested that the branched product would likely be formed due to the preference for placing the Cp ligand in an exocyclic position with respect to the newly formed macrocycle (Scheme 4, II). In contrast, a linear product would force the Cp ligand endocyclic and might be disfavored due to transannular interactions with the bridging macrocycle. However, we were also cognizant that the C9-OH could potentially occupy the open coordination site on the ruthenium catalyst, stabilizing the endocyclic ruthenacyclopentene intermediate and consequently favoring the linear product. Indeed, directing groups proximal to a ruthenacyclopentene are known to have profound effects on linear/branched selectivity as well as reactivity.[31] With this in mind, we started to study this crucial Ru-catalyzed macrocylization.

To examine our key Ru AA coupling, Yamaguchi esterification[32] was first deployed to cleanly join fragments **5** and **14** together, offering ester **18** in 92% yield (Scheme 4, I). Removal of the C9-OTES delivered macrocyclic precursor **19**. To our delight, employing the typical Ru-AA coupling conditions (10 mol% $[RuCp(MeCN)_3]PF_6$, 0.001M acetone, 23°C) [12] provided ~30% conversion with *exclusive* formation of the linear product. It is worth noting that no reaction was observed if the C9-OH was protected as its TES ether (**18**), highlighting the dramatic selectivity effect of a proximal coordinating group. Optimizing the reaction conditions by varying the solvent, temperature, concentration, and catalyst loading further improved the coupling efficiency (see SI, Table S1). To alleviate decomposition issues with the coupling product, the reaction mixture was immediately treated with TESCl before chromatography purification to deliver macrocycle **20** in 39% yield. The subsequent C9-OTES cleavage followed by Dess-Martin oxidation smoothly afforded ketone **21**. Converting ketone **21** into diketone **3** proved unsuccessful: our preliminary results showed that deprotection of the C16-OTroc followed by C14-C15 dihydroxylation worked, but subsequent differentiation of the triols at the C14-16 positions was extremely problematic. Although we were unable to install the α,α'-dihydroxyl ketone moiety, we decided to cleave the C3-OTBS of ketone **21** with HF•pyridine and use the obtained allylic alcohol **22** as an advanced model to investigate the challenging late-stage C4-C5 epoxidation.

Hydroxyl-directed epoxidation has been extensively studied,[33] but this transformation has been problematic in previous synthetic endeavors.[7b] Considering the challenges of this reaction, we first screened a series of epoxidation conditions on a relevant substrate **10**, and promising results were listed in Table 1 (for more details, see SI, Table S2). DMDO[34] gave the undesired chemoselectivity (entry 1), whereas the remaining reagents all preferentially formed epoxide **24**. *m*CPBA provided poor 1.6:1 diastereoselectivity (entry 2).[35] While Sharpless conditions[36] gave no conversion, the modified conditions (without use of chiral ligand)[37] improved the diastereoselectivity to 3:1 (entry 3). Gladly, both $VO(acac)_2$[38] and an optimized Payne epoxidation[39] also delivered good diastereoselectivity (entries 4-5). Next, these conditions (entries 3-5) were applied to macrocycle **22**. Unfortunately, the Payne epoxidation and $VO(acac)_2$ gave no conversion. Ultimately, we found that the modified Sharpless conditions (entry 3) effectively delivered the desired epoxide **23**, albeit as a 1:1 mixture of diastereomers (Scheme 4). The isolated epoxide **23** was unstable, suggesting to us that this allylic epoxidation should be carried out as late as possible.[40]

Table 1. Epoxidation of Diene 10.[a]

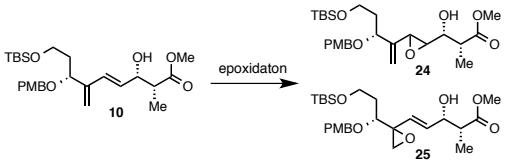

entry	conditions	conv[b]	**24**:**25**[b]	dr (**24**)[b]
1	DMDO	100%	0:100	N/A
2	*m*CPBA	100%	91:9	1.6:1
3	$Ti(OiPr)_4$, TBHP 4Å MS	100%	100:0	3:1
4	$VO(acac)_2$, TBHP 5Å MS	100%	100:0	>1:20
5	3,5-di(CF_3)-benzonitrile H_2O_2, $KHCO_3$	72	88:12	6:1

[a]All reactions were carried out on a 10 mg scale. [b]Conversions, product ratios and diastereoselectivities of **24** were determined by ^1H NMR of the crude reaction mixture.

Overall, during the first generation of our synthetic efforts, we were able to **1)** address the preparation of both southern and northern fragments; **2)** demonstrate the viability of Ru AA coupling and esterification as the key stitching strategy; **3)** achieve a highly chemoselective epoxidation on a complicated late-state macrocyclic compound. In addition, among all the Ru-catalyzed intramolecular alkene-alkyne macrocyclizations, our transformation represents the first example in which a linear product was generated. More importantly, key challenges were identified, including **1)** the current synthetic route of the southern fragment relied on an inefficient enyne metathesis that limited the scalability of the fragment preparation; **2)** the intramolecular Ru AA coupling gave low yield, and improving the coupling efficiency by performing an intermolecular Ru AA coupling that could preclude the competing macrolactionization problem between the C9-OH and C25-OH would be greatly appreciated; **3)** the installation of the α,α'-dihydroxyl ketone moiety through a dihydroxylation method was not achievable, suggesting that we explore a Rubottom oxidation approach.

II. The Second Generation of Synthetic Endeavors

Building upon the foundation laid by our first generation of synthetic endeavors, we first redevised the southern fragment synthesis (Scheme 5). Whereas Marshall coupling[13] was retained to install the propargyl group in the 2nd generation fragment preparation, the enyne metathesis was replaced with a Heck reaction[41] to construct the required diene. Additionally, an asymmetric Mukaiyama aldol reaction[42] was employed to access the *syn* aldol-adduct instead of the Evans aldol reaction.

Scheme 5. Southern Fragment Synthesis (2nd-Gen.)

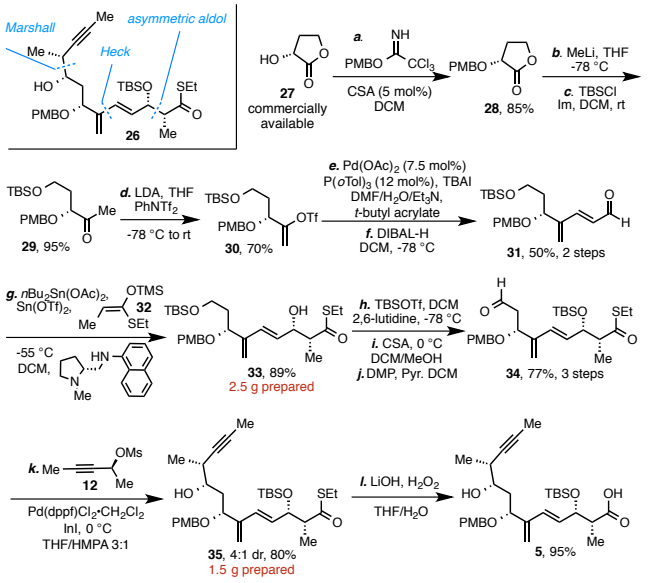

The synthesis of the southern fragment started with masking the commercial alcohol **27** using PMB acetimidate (Scheme 5). The obtained lactone **28** was treated with MeLi followed by TBS-protection to produce methyl ketone **29**, which subsequently underwent kinetic deprotonation and $PhNTf_2$-trapping to give vinyl triflate **30**. Using $Pd(OAc)_2$ and $P(oTol)_3$ under basic aqueous conditions, this vinyl triflate was coupled with *t*-butyl acrylate in a Heck reaction,[41] and the resulting α,β-unsaturated ester was smoothly reduced to aldehyde **31** by slow introduction of DIBAL-H. With this aldehyde in hand, an asymmetric Mukaiyama aldol[42] with silyl enol ether **32** was implemented to afford 2.5 grams of *syn*-adduct **33** in excellent yield. Ensuing TBS-protection of the secondary alcohol, chemoselective removal of the primary TBS ether, and Dess-Martin oxidation[43] delivered aldehyde **34**, which participated in a Marshall coupling[13] with propargyl mesylate **12**[20] to diastereoselectively form homopropargyl alcohol **35**. Overall, 1.5 grams of fragment **35** could be conveniently accessed in 11 steps from commercial materials using our newly designed synthetic approach. Hydrolysis of the thioester using LiOH and H_2O_2 released the free carboxylic acid **5**. The optical rotation and NMR data of this newly prepared acid matched that of compound **5** that was previously synthesized during our first generation of synthetic efforts, therefore confirming the stereoselectivity of our newly developed southern fragment synthesis.

Scheme 6. Northern Fragment Synthesis (2nd-Gen.)

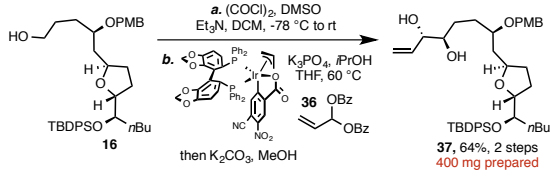

To allow for the installation of the C14-OH via Rubottom oxidation, the northern fragment was modified to a vicinal diol during our 2nd generation of synthetic endeavors (Scheme 6). The starting primary alcohol **16** underwent a Moffatt-Swern oxidation[19] to give an aldehyde intermediate that was further elaborated via a Krische allylation[24] using *gem*-dibenzoate **36** to afford 400 mg of the new northern fragment **37**.

Scheme 7. Assembly of the 2nd-Generation of Southern and Northern Fragments

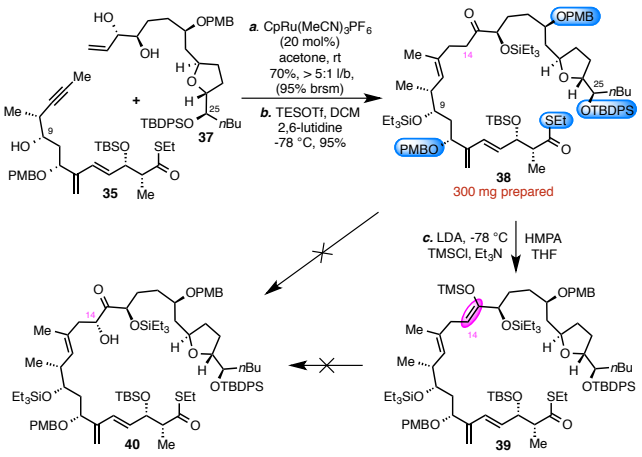

With both fragments **35** and **37** in hand, we started to evaluate the Ru AA coupling (Scheme 7). We wanted to perform this transformation in an intermolecular- rather than intramolecular- fashion to improve the coupling efficiency. To avoid subsequent competing macrolactionization between the C9-OH and C25-OH, we envisioned that the C25-OH could be masked as its TBDPS ether, allowing the C9-OTES to be selectively cleaved and oxidized to the corresponding ketone after Ru AA coupling and C14-OH installation. To our delight, the intermolecular Ru AA coupling significantly improved the yield of this transformation to 70% (for optimization of conditions, see SI, Table S3). The preferentially

Scheme 8. Finalized Synthetic Route Highlighting a Judicious Protecting Group Strategy

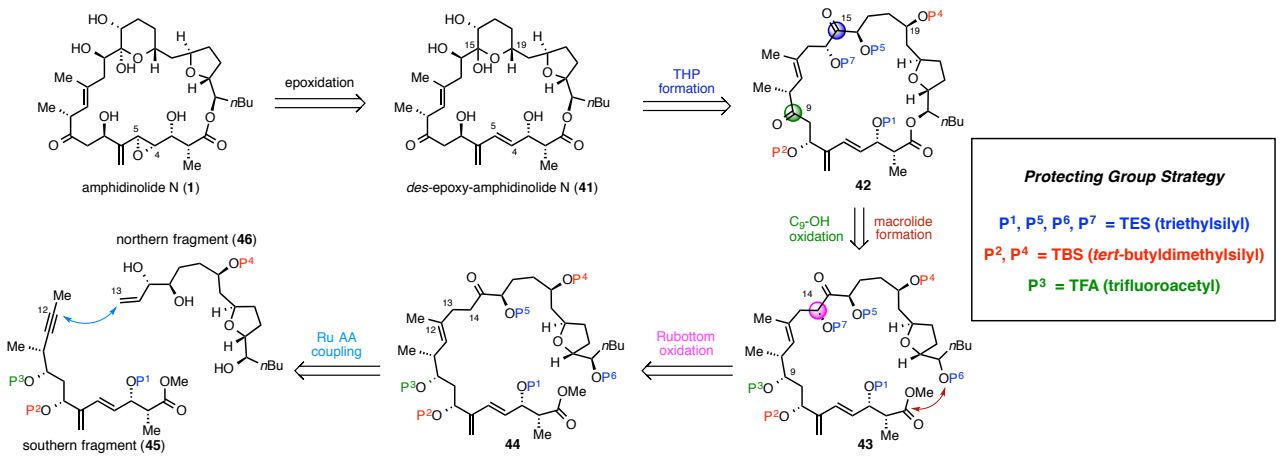

generated linear ketone product was further masked as its TES ether **38**, which was ready for the C14-OH installation. Before exploring the Rubottom oxidation appraoch, a direct conversion of ketone **38** to compound **40** was investigated. Using MoOPH[44] or Davis' reagent[45] with various bases proved fruitless. An α-acyloxylation of ketone **38** using O-benzoyl-*N*-methylhydroxylamine hydrochloride[46] also failed to provide any product **40**, and instead only cleaved the TES protecting groups. As a result, ketone **38** was converted to its TMS enol ether **39** for the subsequent Rubottom oxidation. A variety of oxidants were screened, including *m*CPBA,[10] $MeReO_3$,[47] OsO_4/NMO,[48] DMDO[34] and Davis' reagent.[49] All failed to give promising results and in most cases, the starting enol ether **39** quickly decomposed. We eventually deduced that the thioester did not tolerate these oxidative conditions and was responsible for the decomposition issues, suggesting that we should exchange it for a methyl ester in order to perform the Rubottom oxidation. Meanwhile, another problem arose when attempting cleavage of the TBDPS and the two PMB protecting groups of ketone **38**. Conditions to remove the TBDPS group led to massive decomposition of the starting material **38**. In addition, although unmasking a PMB motif in the presence of a diene moiety is known,[50] cleaving them on ketone **38** under various oxidative[50,51] or Lewis acidic conditions[52] gave disappointing results. These outcomes prompted us to reconsider our whole protecting group strategy.

Overall, during the second generation of our synthetic efforts, we were able to **1)** redesign the synthetic route of the southern fragment, solving the scalability issue; **2)** significantly improve the Ru AA coupling efficiency by performing the reaction in an intermolecular fashion. Meanwhile, some valuable lessons were learnt, including **1)** the thioester should be transformed to a methyl ester in order to carry out the desired Rubottom oxidation; **2)** the PMB and TBDPS protecting groups should be discarded, and the entire protecting group strategy should be carefully and logically devised for easy removal as well as better synthetic efficiency.

III. The Final Generation of Synthetic Endeavors

Taking into account all the successes and shortcomings of the previous two generations, we finalized our synthetic route (Scheme 8). During the first generation, we determined that it would be prudent to perform the feasible allylic epoxidation as late as possible due to the instability of the vinyl epoxide functionality. Based on this, we envisioned a biomimetic epoxidation in the final step, and believed that the C15-OH stereochemistry of *des*-epoxy-amphidinolide N (**41**) would be insignificant due to the equilibratable nature of the hemiacetal. The corresponding THP ring might simultaneously emerge upon deprotection of macrocycle **42**. During the second generation, we learned that the Ru AA coupling efficiency could be drastically enhanced by performing the reaction intermolecularly. Accordingly, to obtain intermediate **42**, fragments **45**-**46** would be stitched together via an intermolecular Ru AA coupling[12] followed by a macrolactonization,[53] alongside a Rubottom oxidation to install the C14-OH.[10] More importantly, a logically designed protecting group strategy was critical. Our synthesis would require: **1)** P^3 to be orthogonal to all other protecting groups for the C9-OH oxidation; **2)** P^1-P^2, P^4-P^5, P^7 of macrocycle **4** to be globally cleavable for step-economy;[54] **3)** P^1 to be removable in the presence of P^2 to direct the C4-C5 epoxidation in case the allylic epoxidation of *des*-epoxy-amphidinolide N (**41**) was non-regioselective.[7b] To satisfy these parameters, TFA was selected for P^3, and the remaining six hydroxyl groups were masked as two sets of silyl ethers.

Scheme 9. Southern Fragment Synthesis (Final-Gen.)

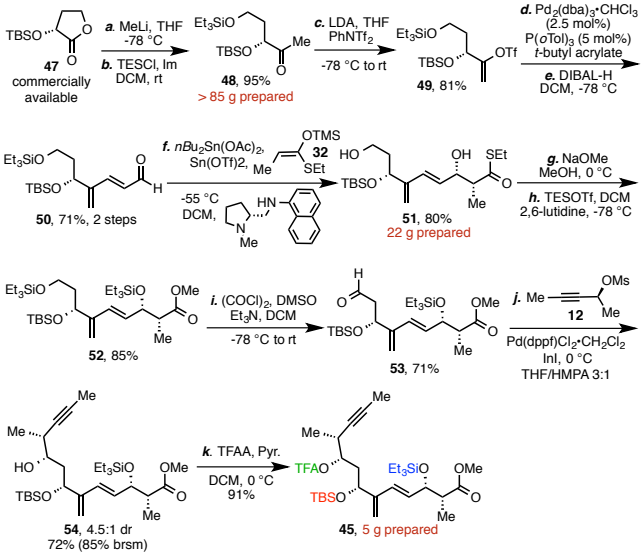

Similar to the second generation southern fragment synthesis, the preparation of fragment **45** began with addition of MeLi to commercial lactone **45**, followed by TES-protection to give methyl

ketone **48** (Scheme 9). Kinetic deprotonation and $PhNTf_2$-trapping delivered vinyl triflate **49**, which subsequently underwent a Heck reaction[41] with *t*-butyl acrylate and a DIBAL-H reduction to afford aldehyde **50**. It is worth noting that using $Pd_2(dba)_3$•$CHCl_3$ rather than $Pd(OAc)_2$ considerably improved the yield of the Heck reaction. Asymmetric Mukaiyama aldol with silyl enol ether **32** produced a total of 22 grams of *syn*-adduct **51**,[42] and the newly introduced thioester was immediately converted to a methyl ester with NaOMe. Use of TESOTf to mask the methyl ester intermediate delivered di-TES ether **52** that was directly transformed into aldehyde **53** by a selective Moffatt-Swern oxidation.[55] Subjecting aldehyde **16** to propargyl mesylate **12**[20] under Marshall conditions diastereoselectively provided homopropargyl alcohol **54**,[13] which upon TFA protection gave southern fragment **45**. Using this robust route, 5 grams of fragment **45** was conveniently prepared in 11 steps with 17% overall yield.

Scheme 10. Northern Fragment Synthesis (Final-Gen.)

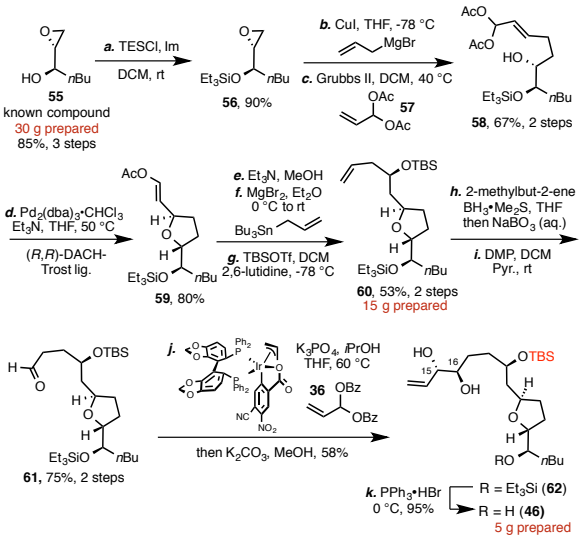

Likewise, the northern fragment **46** commenced with TES-protection of known epoxide **55**, followed by ring opening with allylmagnesium bromide and cross-metastasis with *gem*-diacetate **57** to produce *trans*-olefin **58** (Scheme 10).[7c] The succeeding Pd-AAA diastereoselectively generated the *trans*-THF ring.[25] Treatment of vinyl acetate **59** with Et_3N liberated an aldehyde that participated in Keck allylation[26] and TBS protection to give olefin **60**, the stereochemistry of which was confirmed by converting **60** to its analog **15** via simple protecting-group manipulations. Successive hydroboration/oxidation and Dess-Martin oxidation[43] afforded aldehyde **61**. A Krische allylation using *gem*-dibenzoate **36**[24] was employed to access the desired 1,2-diol **62**, and the stereochemistry of the newly generated C16-OH was verified by converting this alcohol to the corresponding mandelic esters.[21] The C15-OH stereocenter was assigned as *trans* to C16-OH due to the fact that Krische allylation always provides *trans*-diols,[24] but it is worth noting that this C15 stereochemistry is insignificant as it was destroyed in the Ru AA coupling. Selective desilylation of 1,2-diol **62** with PPh_3•HBr[56] ultimately provided 5 grams of northern fragment **46** in 11 steps with 10.5% overall yield.

With both fragments **45** and **46** in hand, the intermolecular Ru AA was carried out (Scheme 11). The immediate product of this coupling, an enol, spontaneously tautomerized to α–hydroxy ketone **63**. Installation of the C14-OH proved extremely challenging. When a direct approach employing MoOPH[44] or Davis' reagent[45] with various bases failed, the Rubottom oxidation was implemented.[10] Subjecting freshly prepared silyl enol ether **64** to *m*CPBA in ethyl acetate or DCM at 0 °C returned to the ketone starting material, whereas $MeReO_3$,[47] OsO_4/NMO,[48] DMDO[34] and Davis' reagent[49] gave either no conversion or complex mixtures. Eventually, we found that a biphasic toluene/pH 7 buffer solvent system and portionwise addition of freshly purified *m*CPBA were crucial to successfully epoxidize silyl enol ether **64**. To suppress decomposition of the siloxy oxirane intermediate during the rearrangement/hydrolysis process, buffered acidic conditions were exploited to afford 1 gram of product **65** as a single diastereomer, the C14-stereochemistry of which was established later (see Figure 2). Subsequent TES protection and TFA cleavage with $NaHCO_3$ liberated the C9-OH, which was oxidized to afford di-ketone **66**. We were gratified to find that the C25-OTES of **66** could be preferentially cleaved in the presence of the C3, C14, and C16 TES ethers by careful introduction of PPh_3•HBr. Exposure of the resultant alcohol **67** to *amano* or *porcine pancreas* lipase in hopes of

Scheme 11. Completion of *des*-epoxy-Amphidinolide N (41)

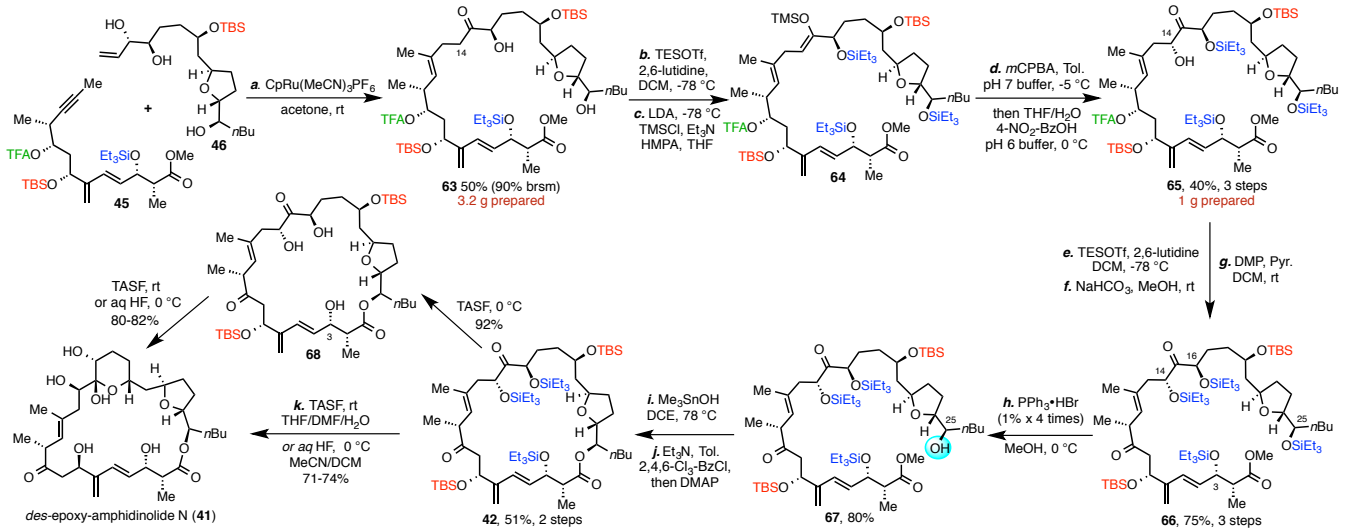

straightforwardly forming macrolactone **42** through intramolecular transesterification was fruitless.[57] Consequently, hydrolysis of ester **67** with Me_3SnOH[23] followed by Yamaguchi esterification[31] was used to yield macrocycle **42**. Subjecting **42** to tris(dimethylamino)sulfonium difluorotrimethylsilicate (TASF)[58] at 0 °C selectively removed three TES groups, leaving both TBS groups untouched. The obtained compound **68** could be used for a C3-OH directed epoxidation. Further deprotection of **68** with extra TASF at ambient temperature or HF at 0 °C occurred concurrently with intramolecular hemiacetal formation at C15-position to generate *des*-epoxy-amphidinolide N (**41**). Alternatively, this compound could be obtained directly from macrocycle **42** upon global deprotection. In both cases, the THP ring formation preferentially produced the same macrolide **41**.

Building upon our previous chemoselective allylic epoxidation results, modified Sharpless epoxidation conditions[37] (Table 1, entry 3) were first applied to *des*-epoxy-amphidinolide N (**41**), but unfortunately the starting material decomposed. Employing $VO(acac)_2$,[38] $VO(OEt)_3$,[59] or Payne conditions[39] gave no conversion. Next, we turned our attention to macrocycle **68** and hoped that use of this macrocycle would alleviate potential chemoselectivity issue. Unluckily, exploiting $VO(acac)_2$,[38] $VO(OEt)_3$,[59] Payne conditions,[39] or Sharpless conditions[36] only returned the starting material, whereas modified Sharpless conditions[37] and $Mo(CO)_6$[60] led to decomposition of the starting material **68**. In addition, use of *m*CPBA[35] afforded complicated results (for details of these efforts, see SI, Table S4). Considering the highly chemoselective allylic epoxidation of macrocycle **22** that was realized in our first generation of synthetic efforts, the current gloomy epoxidation outcomes implied that the allylic epoxidation was highly sensitive to the chemical structure of the macrocycle. We suspected that the conformations of macrocylces **41** and **68**, possibly enforced by intramolecular hydrogen-bonding interactions, might inhibit the desired epoxidation process, leading to the unexpected difficulties in performing the allylic epoxidation at this very late stage.

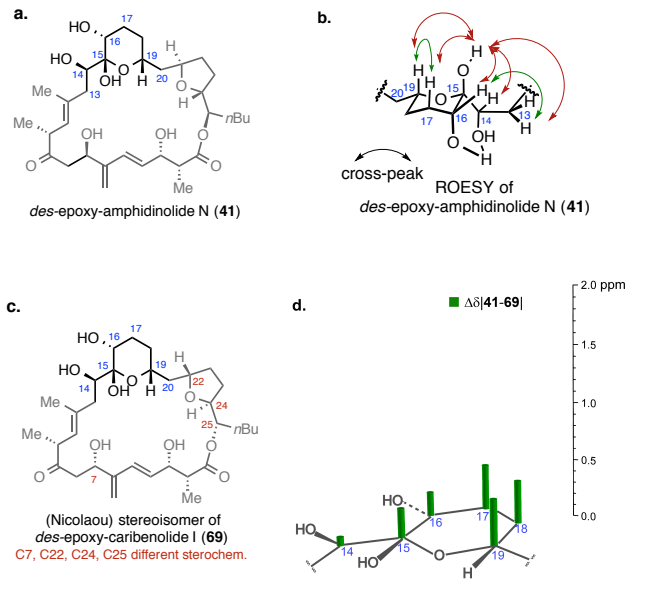

Figure 2. C14-19 structural elucidation of *des*-epoxy-amphidinolide N (**41**). [d]Comparison of *absolute value* of the ^{13}C NMR chemical shift difference at C14-19 between *des*-epoxy-amphidinolide N (**41**) and *des*-epoxy-caribenolide I stereoisomer (**69**). [$\Delta\delta = |\delta\mathbf{41} - \delta\mathbf{69}|$ in ppm]

Nevertheless, the stereochemistry of the THP ring (C14-C19) of *des*-epoxy-amphidinolide N (**41**) was thoroughly investigated using COSY, HSQC, HMBC and ROESY experiments (Figure 2). Clear ROESY cross peaks between the C15-OH and multiple protons at C13, C14, C16, C17 and C19 (Figure 2b, shown in red) suggested that the C15-OH has the orientation indicated in Figure 2a-b. Taking into account the strong ROESY cross peaks between the C17 and C19 protons as well as between the C13 and C16 protons (Figure 2b, shown in green), the conformation of the THP unit (C14-C19) was established, enabling us to further verify the C14 stereochemisty. Interestingly, the observed conformation of the THP ring allows for a stabilizing hydrogen-bonding interaction between C14 and C16 hydroxyl groups (Figure 2b), which is also supported by calculations (see SI). In addition, Nicolaou's *des*-epoxy-caribenolide I stereoisomer (**69**) has identical stereochemistry with our *des*-epoxy-amphidinolide N (**41**) in the THP part (C14-C19) (Figure 2c). Comparing *absolute values* of the ^{13}C NMR chemical shift differences between these two compounds in the C14-19 region revealed trivial variances, all within the range of 0.07-0.41 ppm (Figure 2d). This further supports our structural assignment of *des*-epoxy-amphidinolide N (**41**).

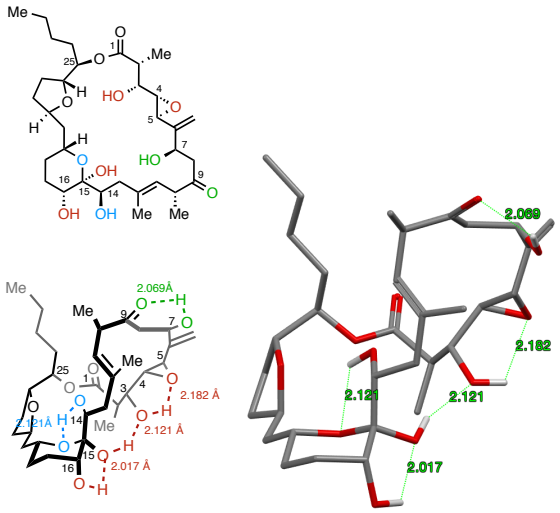

Figure 3. Intramolecular H-bonds of amphidinolide N (**1**) revealed by calculations at the B3LYP/6-31G* level.

Our data shows that C15-OH of *des*-epoxy-amphidinolide N (**41**) has the orientation indicated in Figure 2a-b and that the C14 and C20 side-chains reside in equatorial positions (Figure 2b). In contrast, the C15-OH of amphidinolide N (**1**) bears the opposite stereochemistry, placing the C14 side-chain in an axial position (Figure 3). It is puzzling that the natural product preferentially adopts this apparently less favorable conformation for its THP ring. This phenomenon may be rationalized by intramolecular hydrogen-bonding interactions within amphidinolide N (**1**) that compensate for the energetic penalty for placing the C14 side-chain in an axial position. To further support this idea, conformational optimization of amphidinolide N (**1**) was carried out at the B3LYP/6-31G* level. The results reveal that the C14-hydroxyl proton is 2.121 Å from the THP ring oxygen and the C7-hydroxyl proton is only 2.069 Å away from the neighboring C9-carbonyl, which is consistent with two isolated moderate H-bonds (Figure 3,

left, cyan & green).[61] Similarly, three more modest H-bonds are observed among C16-OH and C15-OH, C15-OH and C3-OH, as well as C3-OH and C4/C5 epoxide (Figure 3, dark-red).[62] Unlike the two isolated H-bonds, these three H-bonds may collaboratively build a hydrogen-bonding bridge across the entire macrocycle to considerably stabilize the adopted conformation.

Additionally, to shed some light on the relationship between amphidinolide N (**1**) and caribenolide I (**2**), we performed NMR experiments using our synthetic *des*-epoxy-amphidinolide (**41**) in both C_6D_6 and CD_2Cl_2, so as to compare our ^{13}C NMR data with that of **1** and **2**. Interestingly, the dissimilarity-pattern of *des*-epoxy-amphidinolide N (**41**) to amphidinolide N (**1**) was in good accordance with that of *des*-epoxy-amphidinolide N (**41**) to caribenolide I (**2**), implying that **1** and **2** could be identical (For further detailed ^{13}C NMR comparisons, see SI, Figure S8). Considering our NMR observations alongside the biogenetic relationship of these two molecules, we conservatively propose that amphidinolide N (**1**) and caribenolide I (**2**) are likely the same molecule.

CONCLUSION

In conclusion, *des*-epoxy-amphidinolide N (**3**) was accomplished in 22 longest linear and 33 total steps. The synthesis took advantage of a convergent design that efficiently joined two fragments with similar levels of structural complexity using a Ru-catalyzed alkene-alkyne coupling and a macrolactonization. Three generations of synthetic endeavors were reported. The first generation validated the key Ru AA coupling stitching strategy and realized a challenging chemoselective allylic epoxidation of a complex macrocycle, but left installation of the α,α'-dihydroxy ketone moiety and scalable preparation of the southern fragment as unanswered questions. The second generation addressed the scalability of the southern fragment synthesis and significantly improved the Ru AA coupling efficiency, but revealed that the thioether was incompatible with the Rubottom oxidation alongside the deprotection troubles. Evolving from these two generations of synthetic efforts, the final generation not only logically designed the whole protecting group strategy, but also successfully installed the C14-OH via a carefully tuned Rubottom oxidation, allowing us to realize the synthesis of *des*-epoxy-amphidinolide N. Several remarkable asymmetric transition-metal-catalyzed reactions were deployed, including Mukaiyama aldol (Sn), Marshall coupling (Pd-In), Pd-AAA (Pd), and Krische allylation (Ir). Structural elucidation of the THP ring of *des*-epoxy-amphidinolide N (**41**) not only verified our assignments but also led us to disclose the hydrogen-bonding network in amphidinolide N (**1**). Comparisons of ^{13}C NMR chemical shift differences using our synthetic *des*-epoxy-amphidinolide N (**41**) suggest that amphidinolide N (**1**) and carbenolide I (**2**) are possibly the same chemical entity.

ASSOCIATED CONTENT

Supporting Information

The Supporting Information is available free of charge on the ACS Publications website.

Experimental and computational details, compound characterization data, and spectra (PDF)

AUTHOR INFORMATION

Corresponding Author

*bmtrost@stanford.edu

ACKNOWLEDGMENT

We thank Prof. J. Du Bois for providing a Shigemi tube, Dr. T. Kakeshpour for computational discussion, Dr. S. Lynch for assistance with NMR spectroscopy, and C. A. Kalnmals for critical reading of the manuscript. C.E.S. is the recipient of an NIH Ruth L. Kirschstein National Research Service Award (GM101747). C.P. and M.H. are the recipients of DAAD fellowships (ISAP and DE1243257 respectively).

REFERENCES

1. For some recent examples of biological evulation of macrolide and their analogues, see: (a) Ketcham, J. M.; Volchkov, I.; Chen, T.-Y.; Blumberg, P. M.; Kedei, N.; Lewin, N. E.; Krische, M. J. Evaluation of Chromane-Based Bryostatin Analogues Prepared via Hydrogen-Mediated C–C Bond Formation: Potency Does Not Confer Bryostatin-like Biology. *J. Am. Chem. Soc.* **2016,** *138*, 13415; (b) Nicolaou, K. C.; Rhoades, D.; Wang, Y.; Bai, R.; Hamel, E.; Aujay, M.; Sandoval, J.; Gavrilyuk, J. 12,13-Aziridinyl Epothilones. Stereoselective Synthesis of Trisubstituted Olefinic Bonds from Methyl Ketones and Heteroaromatic Phosphonates and Design, Synthesis, and Biological Evaluation of Potent Antitumor Agents. *J. Am. Chem. Soc.* **2017,** *139*, 7318.
2. For some rencent examples of synthesis of macrocyclic natural products, see: (a) Bai, Y.; Shen, X.; Li, Y.; Dai, M. Total Synthesis of (−)-Spinosyn A via Carbonylative Macrolactonization. *J. Am. Chem. Soc.* **2016,** *138*, 10838; (b) Nguyen, M. H.; Imanishi, M.; Kurogi, T.; Smith, A. B. Total Synthesis of (−)-Mandelalide A Exploiting Anion Relay Chemistry (ARC): Identification of a Type II ARC/CuCN Cross-Coupling Protocol. *J. Am. Chem. Soc.* **2016,** *138*, 3675; (c) Shin, I.; Hong, S.; Krische, M. J. Total Synthesis of Swinholide A: An Exposition in Hydrogen-Mediated C–C Bond Formation. *J. Am. Chem. Soc.* **2016,** *138*, 14246; (d) Wang, G.; Krische, M. J. Total Synthesis of (+)-SCH 351448: Efficiency via Chemoselectivity and Redox-Economy Powered by Metal Catalysis. *J. Am. Chem. Soc.* **2016,** *138*, 8088; (e) Williams, S.; Jin, J.; Kan, S. B. J.; Li, M.; Gibson, L. J.; Paterson, I. An Expedient Total Synthesis of Chivosazole F: an Actin-Binding Antimitotic Macrolide from the Myxobacterium Sorangium Cellulosum. *Angew. Chem. Int. Ed.* **2016,** *56*, 645; (f) Nicolaou, K. C.; Bellavance, G.; Buchman, M.; Pulukuri, K. K. Total Syntheses of Disorazoles A1 and B1 and Full Structural Elucidation of Disorazole B1. *J. Am. Chem. Soc.* **2017,** *139*, 15636; (g) Zhuo, C.-X.; Fürstner, A. Catalysis-Based Total Syntheses of Pateamine A and DMDA-Pat A. *J. Am. Chem. Soc.* **2018,** *140*, 10514.
3. For some rencent examples of synthesis of macrolide analogues, see: (a) Andrews, I. P.; Ketcham, J. M.; Blumberg, P. M.; Kedei, N.; Lewin, N. E.; Peach, M. L.; Krische, M. J. Synthesis of seco-B-Ring Bryostatin Analogue WN-1 via C–C Bond-Forming Hydrogenation: Critical Contribution of the B-Ring in Determining Bryostatin-like and Phorbol 12-Myristate 13-Acetate-like Properties. *J. Am. Chem. Soc.* **2014,** *136*, 13209; (b) Zhuo, C.-X.; Fürstner, A. Concise Synthesis of a Pateamine A Analogue with In Vivo Anticancer Activity Based on an Iron-Catalyzed Pyrone Ring Opening/Cross-Coupling. *Angew. Chem. Int. Ed.* **2016,** *55*, 6051; (c) Anderl, F.; Größl, S.; Wirtz, C.; Fürstner, A. Total Synthesis of Belizentrin Methyl Ester: Report on a Likely Conquest. *Angew. Chem. Int. Ed.* **2018,** *57*, 10712.
4. For reviews of amphidinolides, see: (a) Kobayashi, J. i.; Tsuda, M. Amphidinolides, bioactive macrolides from symbiotic marine dinoflagellates. *Nat. Prod. Rep.* **2004,** *21*, 77; (b) Kobayashi, J. i.; Kubota, T. Bioactive Macrolides and Polyketides from Marine Dinoflagellates of the Genus Amphidinium. *J. Nat. Prod.* **2007,** *70*, 451; (c) Kobayashi, J. i. Amphidinolides and Its Related Macrolides from Marine Dinoflagellates. *J. Antibiot.* **2008,** *61*, 271; (d) Fürstner, A. From Total Synthesis to Diverted Total Synthesis: Case Studies in the Amphidinolide Series. *Isr. J. Chem.* **2011,** *51*, 329.

5. (a) Ishibashi, M.; Yamaguchi, N.; Sasaki, T.; Kobayashi, J. i. Amphidinolide N, a novel 26-membered macrolide with remarkably potent cytotoxicity from the cultured marine dinoflagellate Amphidinium sp. *J. Chem. Soc., Chem. Commun.* **1994**, 1455; (b) Takahashi, Y.; Kubota, T.; Imachi, M.; Wälchli, M. R.; Kobayashi, J. i. Revised structure and stereochemical assignments of amphidinolide N. *J. Antibiot.* **2013,** *66*, 277.
6. For synthesis of amphidinolide F, see: (a) Mahapatra, S.; Carter, R. G. Enantioselective Total Synthesis of Amphidinolide F. *Angew. Chem. Int. Ed.* **2012,** *51*, 7948; (b) Mahapatra, S.; Carter, R. G. Exploiting Hidden Symmetry in Natural Products: Total Syntheses of Amphidinolides C and F. *J. Am. Chem. Soc.* **2013,** *135*, 10792; (c) Valot, G.; Regens, C. S.; O'Malley, D. P.; Godineau, E.; Takikawa, H.; Fürstner, A. Total Synthesis of Amphidinolide F. *Angew. Chem. Int. Ed.* **2013,** *52*, 9534; (d) Valot, G.; Mailhol, D.; Regens, C. S.; O'Malley, D. P.; Godineau, E.; Takikawa, H.; Philipps, P.; Fürstner, A. Concise Total Syntheses of Amphidinolides C and F. *Chem. Eur. J.* **2014,** *21*, 2398; (e) Ferrié, L.; Fenneteau, J.; Figadère, B. Total Synthesis of the Marine Macrolide Amphidinolide F. *Org. Lett.* **2018,** *20*, 3192.
7. For synthetic studies, see: (a) Nicolaou, K. C.; Brenzovich, W. E.; Bulger, P. G.; Francis, T. M. Synthesis of iso-epoxy-amphidinolide N and des-epoxy-caribenolide I structures. Initial forays. *Org. Biomol. Chem.* **2006,** *4*, 2119; (b) Nicolaou, K. C.; Bulger, P. G.; Brenzovich, W. E. Synthesis of iso-epoxy-amphidinolide N and des-epoxy-caribenolide I structures. Revised strategy and final stages. *Org. Biomol. Chem.* **2006,** *4*, 2158; (c) Trost, B. M.; Rey, J. Diastereoselective Formation of Tetrahydrofurans via Pd-Catalyzed Asymmetric Allylic Alkylation: Synthesis of the C13–C29 Subunit of Amphidinolide N. *Org. Lett.* **2012,** *14*, 5632; (d) Fujishima, Y.; Ogura, Y.; Towada, R.; Enomoto, M.; Kuwahara, S. Stereoselective synthesis of the C17–C29 fragment of amphidinolide N. *Tetrahedron Lett.* **2016,** *57*, 5240; (e) Kawashima, Y.; Toyoshima, A.; Fuwa, H.; Sasaki, M. Toward the Total Synthesis of Amphidinolide N: Synthesis of the C8–C29 Fragment. *Org. Lett.* **2016,** *18*, 2232; (f) Ochiai, K.; Kuppusamy, S.; Yasui, Y.; Harada, K.; Gupta, N. R.; Takahashi, Y.; Kubota, T.; Kobayashi, J. i.; Hayashi, Y. Total Synthesis of the 7,10-Epimer of the Proposed Structure of Amphidinolide N, Part II: Synthesis of C17–C29 Subunit and Completion of the Synthesis. *Chem. Eur. J.* **2016,** *22*, 3287; (g) Ochiai, K.; Kuppusamy, S.; Yasui, Y.; Okano, T.; Matsumoto, Y.; Gupta, N. R.; Takahashi, Y.; Kubota, T.; Kobayashi, J. i.; Hayashi, Y. Total Synthesis of the 7,10-Epimer of the Proposed Structure of Amphidinolide N, Part I: Synthesis of the C1–C13 Subunit. *Chem. Eur. J.* **2016,** *22*, 3282; (h) Toyoshima, A.; Sasaki, M. Toward a total synthesis of amphidinolide N: convergent synthesis of the C1–C13 segment. *Tetrahedron Lett.* **2016,** *57*, 3532.
8. Bauer, I.; Maranda, L.; Young, K. A.; Shimizu, Y.; Fairchild, C.; Cornell, L.; MacBeth, J.; Huang, S. Isolation and Structure of Caribenolide I, a Highly Potent Antitumor Macrolide from a Cultured Free-Swimming Caribbean Dinoflagellate, Amphidinium sp. S1-36-5. *J. Org. Chem.* **1995,** *60*, 1084.
9. (a) Kolb, H. C.; VanNieuwenhze, M. S.; Sharpless, K. B. Catalytic Asymmetric Dihydroxylation. *Chem. Rev.* **1994,** *94*, 2483; (b) Cha, J. K.; Kim, N.-S. Acyclic Stereocontrol Induced by Allylic Alkoxy Groups. Synthetic Applications of Stereoselective Dihydroxylation in Natural Product Synthesis. *Chem. Rev.* **1995,** *95*, 1761.
10. Rubottom, G. M.; Vazquez, M. A.; Pelegrina, D. R. Peracid oxidation of trimethylsilyl enol ethers: A facile α-hydroxylation procedure. *Tetrahedron Lett.* **1974,** *15*, 4319.
11. Trost, B. M. The atom economy-a search for synthetic efficiency. *Science* **1991,** *254*, 1471.
12. (a) Trost, B. M.; Dean Toste, F. A new Ru catalyst for alkene-alkyne coupling. *Tetrahedron Lett.* **1999,** *40*, 7739; (b) Trost, B. M.; Toste, F. D.; Pinkerton, A. B. Non-Metathesis Ruthenium-Catalyzed C–C Bond Formation. *Chem. Rev.* **2001,** *101*, 2067; (c) Trost, B. M.; Frederiksen, M. U.; Rudd, M. T. Ruthenium-Catalyzed Reactions—A Treasure Trove of Atom-Economic Transformations. *Angew. Chem. Int. Ed.* **2005,** *44*, 6630.
13. (a) Marshall, J. A.; Grant, C. M. Preparation of Chiral Allenylmetal Reagents from Enantioenriched Allenyl Iodides and Propargylic Mesylates. A Comparison of Indium, Bismuth, and Tin Derivatives. *J. Org. Chem.* **1999,** *64*, 8214; (b) Marshall, J. A.; Chobanian, H. R.; Yanik, M. M. Lipase-Mediated Resolution of 4-TMS-3-butyn-2-ol and Use of the Mesylate Derivatives as a Precursor to a Highly Stereoselective Chiral Allenylindium Reagent. *Org. Lett.* **2001,** *3*, 3369.
14. Diver, S. T.; Giessert, A. J. Enyne Metathesis (Enyne Bond Reorganization). *Chem. Rev.* **2004,** *104*, 1317.
15. Gage, J. R.; Evans, D. A. DiastereoselectiveAldol Condensation Using a Chiral Oxazolidinone Auxiliary: (2S*,3S*)-3-Hydroxy-3-phenyl-2-methylpropanoic Acid. *Org. Synth.* **1990,** *68*, 83.
16. Gung, B. W.; Fox, R. M. Total synthesis of bidensyneosides A2 and C: remarkable protecting group effects in glycosylation. *Tetrahedron* **2004,** *60*, 9405.
17. Clark, J. R.; Diver, S. T. Atom Economy in the Metathesis Cross-Coupling of Alkenes and Alkynes. *Org. Lett.* **2011,** *13*, 2896.
18. (a) Dias, E. L.; Nguyen, S. T.; Grubbs, R. H. Well-Defined Ruthenium Olefin Metathesis Catalysts: Mechanism and Activity. *J. Am. Chem. Soc.* **1997,** *119*, 3887; (b) Voigtritter, K.; Ghorai, S.; Lipshutz, B. H. Rate Enhanced Olefin Cross-Metathesis Reactions: The Copper Iodide Effect. *J. Org. Chem.* **2011,** *76*, 4697.
19. (a) Omura, K.; Swern, D. Oxidation of alcohols by "activated" dimethyl sulfoxide. a preparative, steric and mechanistic study. *Tetrahedron* **1978,** *34*, 1651; (b) Mancuso, A. J.; Brownfain, D. S.; Swern, D. Structure of the dimethyl sulfoxide-oxalyl chloride reaction product. Oxidation of heteroaromatic and diverse alcohols to carbonyl compounds. *J. Org. Chem.* **1979,** *44*, 4148.
20. Muri, D.; Carreira, E. M. Stereoselective Synthesis of Erythronolide A via Nitrile Oxide Cycloadditions and Related Studies. *J. Org. Chem.* **2009,** *74*, 8695.
21. Trost, B. M.; Belletire, J. L.; Godleski, S.; McDougal, P. G.; Balkovec, J. M.; Baldwin, J. J.; Christy, M. E.; Ponticello, G. S.; Varga, S. L.; Springer, J. P. On the Use of O-Methylmandelic Acid for Establishment of Absolute Configuration of secondary Alcohols. *J. Org. Chem.* **1986,** *51*, 2370.
22. Trost, B. M.; Ball, Z. T. Intramolecular Endo-Dig Hydrosilylation Catalyzed by Ruthenium: Evidence for a New Mechanistic Pathway. *J. Am. Chem. Soc.* **2003,** *125*, 30.
23. Nicolaou, K. C.; Estrada, A. A.; Zak, M.; Lee, S. H.; Safina, B. S. A Mild and Selective Method for the Hydrolysis of Esters with Trimethyltin Hydroxide. *Angew. Chem. Int. Ed.* **2005,** *44*, 1378.
24. (a) Han, S. B.; Han, H.; Krische, M. J. Diastereo- and Enantioselective anti-Alkoxyallylation Employing Allylic gem-Dicarboxylates as Allyl Donors via Iridium-Catalyzed Transfer Hydrogenation. *J. Am. Chem. Soc.* **2010,** *132*, 1760; For reviews of Krische allylation, see: (b) Hassan, A.; Krische, M. J. Unlocking Hydrogenation for C–C Bond Formation: A Brief Overview of Enantioselective Methods. *Org. Proc. Res. Dev.* **2011,** *15*, 1236; (c) Ketcham, J. M.; Shin, I.; Montgomery, T. P.; Krische, M. J. Catalytic Enantioselective C-H Functionalization of Alcohols by Redox-Triggered Carbonyl Addition: Borrowing Hydrogen, Returning Carbon. *Angew. Chem. Int. Ed.* **2014,** *53*, 9142; (d) Feng, J.; Kasun, Z. A.; Krische, M. J. Enantioselective Alcohol C–H Functionalization for Polyketide Construction: Unlocking Redox-Economy and Site-Selectivity for Ideal Chemical Synthesis. *J. Am. Chem. Soc.* **2016,** *138*, 5467; (e) Kim, S. W.; Zhang, W.; Krische, M. J. Catalytic Enantioselective Carbonyl Allylation and Propargylation via Alcohol-Mediated Hydrogen Transfer: Merging the Chemistry of Grignard and Sabatier. *Acc. Chem. Res.* **2017,** *50*, 2371.
25. Trost, B. M. Pd- and Mo-Catalyzed Asymmetric Allylic Alkylation. *Org. Proc. Res. Dev.* **2012,** *16*, 185.
26. Keck, G. E.; Castellino, S.; Wiley, M. R. Dramatic effects of oxygen substituents on 1,3-asymmetric induction in additions of allyltriphenylstannane to .beta.-alkoxy aldehydes: a chemical and spectroscopic investigation. *J. Org. Chem.* **1986,** *51*, 5478.
27. (a) Trost, B. M.; Stivala, C. E.; Hull, K. L.; Huang, A.; Fandrick, D. R. A Concise Synthesis of (−)-Lasonolide A. *J. Am. Chem. Soc.* **2014,**

136, 88; (b) Trost, B. M.; Stivala, C. E.; Fandrick, D. R.; Hull, K. L.; Huang, A.; Poock, C.; Kalkofen, R. Total Synthesis of (−)-Lasonolide A. *J. Am. Chem. Soc.* **2016,** *138*, 11690.

28. (a) Trost, B. M.; Chisholm, J. D.; Wrobleski, S. T.; Jung, M. Ruthenium-Catalyzed Alkene-Alkyne Coupling: Synthesis of the Proposed Structure of Amphidinolide A. *J. Am. Chem. Soc.* **2002**, *124*, 12420; (b) Trost, B. M.; Harrington, P. E. Structure Elucidation of (+)-Amphidinolide A by Total Synthesis and NMR Chemical Shift Analysis. *J. Am. Chem. Soc.* **2004,** *126*, 5028; (c) Trost, B. M.; Harrington, P. E.; Chisholm, J. D.; Wrobleski, S. T. Total Synthesis of (+)-Amphidinolide A. Structure Elucidation and Completion of the Synthesis. *J. Am. Chem. Soc.* **2005,** *127*, 13598; (d) Trost, B. M.; Wrobleski, S. T.; Chisholm, J. D.; Harrington, P. E.; Jung, M. Total Synthesis of (+)-Amphidinolide A. Assembly of the Fragments. *J. Am. Chem. Soc.* **2005,** *127*, 13589.
29. Nakamura, S.; Kikuchi, F.; Hashimoto, S. Total Synthesis of Pinnatoxin A. *Angew. Chem. Int. Ed.* **2008,** *47*, 7091.
30. (a) Trost, B. M.; Amans, D.; Seganish, W. M.; Chung, C. K. Total Synthesis of Laulimalide: Assembly of the Fragments and Completion of the Synthesis of the Natural Product and a Potent Analogue. *Chem. Eur. J.* **2012,** *18*, 2961; (b) Trost, B. M.; Seganish, W. M.; Chung, C. K.; Amans, D. Total Synthesis of Laulimalide: Synthesis of the Northern and Southern Fragments. *Chem. Eur. J.* **2012,** *18*, 2948.
31. (a) Trost, B. M.; Cregg, J. J. Ruthenium-Catalyzed Alkene–Alkyne Coupling of Disubstituted Olefins: Application to the Stereoselective Synthesis of Trisubstituted Enecarbamates. *J. Am. Chem. Soc.* **2015,** *137*, 620; (b) Rummelt, S. M.; Cheng, G.-J.; Gupta, P.; Thiel, W.; Fürstner, A. Hydroxy-Directed Ruthenium-Catalyzed Alkene/Alkyne Coupling: Increased Scope, Stereochemical Implications, and Mechanistic Rationale. *Angew. Chem. Int. Ed.* **2017,** *56*, 3599; (c) Trost, B. M.; Sharif, E. U.; Cregg, J. J. Ru-catalyzed sequence for the synthesis of cyclic amido-ethers. *Chem. Sci.* **2017,** *8*, 770.
32. Inanaga, J.; Hirata, K.; Saeki, H.; Katsuki, T.; Yamaguchi, M. A Rapid Esterification by Means of Mixed Anhydride and Its Application to Large-ring Lactonization. *Bull. Chem. Soc. Jpn.* **1979,** *52*, 1989.
33. (a) Hoveyda, A. H.; Evans, D. A.; Fu, G. C. Substrate-directable chemical reactions. *Chem. Rev.* **1993,** *93*, 1307; (b) Adam, W.; Wirth, T. Hydroxy Group Directivity in the Epoxidation of Chiral Allylic Alcohols: Control of Diastereoselectivity through Allylic Strain and Hydrogen Bonding. *Acc. Chem. Res.* **1999,** *32*, 703.
34. Murray, R. W. Chemistry of dioxiranes. 12. Dioxiranes. *Chem. Rev.* **1989,** *89*, 1187.
35. Bradley, L. M.; Springer, J. W.; Delate, G. M.; Goodman, A. Epoxidation of Geraniol: An Advanced Organic Experiment that Illustrates Asymmetric Synthesis. *J. Chem. Educ.* **1997,** *74*, 1336.
36. (a) Sharpless, K. B.; Verhoeven, T. R. Metal-Catalyzed, Highly Selective Oxygenations of Olefins and Acetylenes with *tert*-Butyl Hydroperoxide. Practical Considerations and Mechanisms. *Aldrichimica Acta* **1979**, *12*, 63; (b) Rossiter, B. E.; Verhoeven, T. R.; Sharpless, K. B. Stereoselective epoxidation of acyclic allylic alcohols. A correction of our previous work. *Tetrahedron Lett.* **1979,** *20*, 4733; (c) Paterson, I.; De Savi, C.; Tudge, M. Total Synthesis of the Microtubule-Stabilizing Agent (−)-Laulimalide. *Org. Lett.* **2001,** *3*, 3149; (d) Kanoh, N.; Kawamata, A.; Itagaki, T.; Miyazaki, Y.; Yahata, K.; Kwon, E.; Iwabuchi, Y. A Concise and Unified Strategy for Synthesis of the C1–C18 Macrolactone Fragments of FD-891, FD-892 and Their Analogues: Formal Total Synthesis of FD-891. *Org. Lett.* **2014,** *16*, 5216.
37. Lu, L.; Zhang, W.; Nam, S.; Horne, D. A.; Jove, R.; Carter, R. G. Amphidinolide B: Total Synthesis, Structural Investigation, and Biological Evaluation. *J. Org. Chem.* **2013,** *78*, 2213.
38. Itoh, T.; Jitsukawa, K.; Kaneda, K.; Teranishi, S. Vanadium-catalyzed epoxidation of cyclic allylic alcohols. Stereoselectivity and stereocontrol mechanism. *J. Am. Chem. Soc.* **1979,** *101*, 159.
39. Payne, G. B. A simplified procedure for epoxidation by benzonitrile-hydrogen peroxide. Selective oxidation of 2-allylcyclohexanone. *Tetrahedron* **1962,** *18*, 763.
40. It is worth mentioning that the vinyl epoxide unit flanked by a masked hydroxy group in amphidinolide V or the simple protected hydroxy epoxide motif in amphidinolides K and P is relatively stable, see: (a) Fürstner, A.; Larionov, O.; Flügge, S. What is Amphidinolide V? Report on a Likely Conquest. *Angew. Chem. Int. Ed.* **2007,** *46*, 5545; (b) Fürstner, A.; Flügge, S.; Larionov, O.; Takahashi, Y.; Kubota, T.; Kobayashi, J. Total Synthesis and Biological Evaluation of Amphidinolide V and Analogues. *Chem. Eur. J.* **2009,** *15*, 4011; (c) Volchkov, I.; Lee, D. Asymmetric Total Synthesis of (−)-Amphidinolide V through Effective Combinations of Catalytic Transformations. *J. Am. Chem. Soc.* **2013,** *135*, 5324; (d) Williams, D. R.; Meyer, K. G. Total Synthesis of (+)-Amphidinolide K. *J. Am. Chem. Soc.* **2001,** *123*, 765; (e) Williams, D. R.; Myers, B. J.; Mi, L. Total Synthesis of (−)-Amphidinolide P *Org. Lett.* **2000,** *2*, 945; (f) Trost, B. M.; Papillon, J. P. N. Alkene-Alkyne Coupling as a Linchpin: An Efficient and Convergent Synthesis of Amphidinolide P. *J. Am. Chem. Soc.* **2004,** *126*, 13618.
41. Heck, R. F.; Nolley, J. P. Palladium-catalyzed vinylic hydrogen substitution reactions with aryl, benzyl, and styryl halides. *J. Org. Chem.* **1972,** *37*, 2320.
42. Kobayashi, S.; Uchiro, H.; Fujishita, Y.; Shiina, I.; Mukaiyama, T. Asymmetric aldol reaction between achiral silyl enol ethers and achiral aldehydes by use of a chiral promoter system. *J. Am. Chem. Soc.* **1991,** *113*, 4247.
43. Dess, D. B.; Martin, J. C. Readily accessible 12-I-5 oxidant for the conversion of primary and secondary alcohols to aldehydes and ketones. *J. Org. Chem.* **1983,** *48*, 4155.
44. Vedejs, E.; Engler, D. A.; Telschow, J. E. Transition-metal peroxide reactions. Synthesis of .alpha.-hydroxycarbonyl compounds from enolates. *J. Org. Chem.* **1978,** *43*, 188.
45. Davis, F. A.; Vishwakarma, L. C.; Billmers, J. G.; Finn, J. Synthesis of .alpha.-hydroxycarbonyl compounds (acyloins): direct oxidation of enolates using 2-sulfonyloxaziridines. *J. Org. Chem.* **1984,** *49*, 3241.
46. Beshara, C. S.; Hall, A.; Jenkins, R. L.; Jones, K. L.; Jones, T. C.; Killeen, N. M.; Taylor, P. H.; Thomas, S. P.; Tomkinson, N. C. O. A General Method for the α-Acyloxylation of Carbonyl Compounds. *Org. Lett.* **2005,** *7*, 5729.
47. Stanković, S.; Espenson, J. H. Oxidation of Methyl Trimethylsilyl Ketene Acetals to α-Hydroxyesters with Urea Hydrogen Peroxide Catalyzed by Methyltrioxorhenium. *J. Org. Chem.* **2000,** *65*, 5528.
48. McCormick, J. P.; Tomasik, W.; Johnson, M. W. α-Hydroxylation of ketones: Osmium tetroxide/N-methylmorpholine-N-oxide oxidation of silyl enol ethers. *Tetrahedron Lett.* **1981,** *22*, 607.
49. Davis, F. A.; Sheppard, A. C. Oxidation of silyl enol ethers using 2-sulfonyloxaziridines. Synthesis of .alpha.-siloxy epoxides and .alpha.-hydroxy carbonyl compounds. *J. Org. Chem.* **1987,** *52*, 954.
50. (a) Paterson, I.; Davies, R. D. M.; Marquez, R. Total Synthesis of the Callipeltoside Aglycon. *Angew. Chem. Int. Ed.* **2001,** *40*, 603; (b) Paterson, I.; Davies, R. D. M.; Heimann, A. C.; Marquez, R.; Meyer, A. Stereocontrolled Total Synthesis of (−)-Callipeltoside A. *Org. Lett.* **2003,** *5*, 4477; (c) Hara, A.; Morimoto, R.; Iwasaki, Y.; Saitoh, T.; Ishikawa, Y.; Nishiyama, S. Total Syntheses of Amphidinolides B, G, and H. *Angew. Chem. Int. Ed.* **2012,** *51*, 9877.
51. Kronenthal, D. R.; Han, C. Y.; Taylor, M. K. Oxidative N-dearylation of 2-azetidinones. p-Anisidine as a source of azetidinone nitrogen. *J. Org. Chem.* **1982,** *47*, 2765.
52. (a) Bouzide, A.; Sauvé, G. Lewis Acid-Catalyzed Deprotection of p-Methoxybenzyl Ether. *Synlett* **1997**, 1153; (b) Cappa, A.; Marcantoni, E.; Torregiani, E.; Bartoli, G.; Bellucci, M. C.; Bosco, M.; Sambri, L. A Simple Method for the Selective Deprotection of p-Methoxybenzyl Ethers by Cerium(III) Chloride Heptahydrate and Sodium Iodide. *J. Org. Chem.* **1999,** *64*, 5696; (c) Falck, J. R.; Barma, D. K.; Baati, R.; Mioskowski, C. Differential Cleavage of Arylmethyl Ethers: Reactivity of 2,6-Dimethoxybenzyl Ethers. *Angew. Chem. Int. Ed.* **2001,** *40*, 1281.
53. Li, Y.; Yin, X.; Dai, M. Catalytic macrolactonizations for natural product synthesis. *Nat. Prod. Rep.* **2017,** *34*, 1185.

54. Wender, P. A.; Verma, V. A.; Paxton, T. J.; Pillow, T. H. Function-Oriented Synthesis, Step Economy, and Drug Design. *Acc. Chem. Res.* **2008,** *41*, 40.
55. Rodríguez, A.; Nomen, M.; Spur, B. W.; Godfroid, J. J. Selective oxidation of primary silyl ethers and its application to the synthesis of natural products. *Tetrahedron Lett.* **1999,** *40*, 5161.
56. Heathcock, C. H.; McLaughlin, M.; Medina, J.; Hubbs, J. L.; Wallace, G. A.; Scott, R.; Claffey, M. M.; Hayes, C. J.; Ott, G. R. Multigram Synthesis of the C29–C51 Subunit and Completion of the Total Synthesis of Altohyrtin C (Spongistatin 2). *J. Am. Chem. Soc.* **2003,** *125*, 12844.
57. Makita, A.; Nihira, T.; Yamada, Y. Lipase catalyzed synthesis of macrocyclic lactones in organic solvents. *Tetrahedron Lett.* **1987,** *28*, 805.
58. Scheidt, K. A.; Chen, H.; Follows, B. C.; Chemler, S. R.; Coffey, D. S.; Roush, W. R. Tris(dimethylamino)sulfonium Difluorotrimethylsilicate, a Mild Reagent for the Removal of Silicon Protecting Groups. *J. Org. Chem.* **1998**, *63*, 6436.
59. (a) Nicolaou, K. C.; Harrison, S. T. Total Synthesis of Abyssomicin C and atrop-Abyssomicin C. *Angew. Chem. Int. Ed.* **2006,** *45*, 3256; (b) Kuroda, Y.; Nicacio, K. J.; Alves da Silva-Jr, I.; Leger, P. R.; Chang, S.; Gubiani, J. R.; Deflon, V. M.; Nagashima, N.; Rode, A.; Blackford, K.; Ferreira, A. G.; Sette, L. D.; Williams, D. E.; Andersen, R. J.; Jancar, S.; Berlinck, R. G. S.; Sarpong, R. Isolation, synthesis and bioactivity studies of phomactin terpenoids. *Nat. Chem.* **2018**, *10*, 938.
60. Sharpless, K. B.; Michaelson, R. C. High stereo- and regioselectivities in the transition metal catalyzed epoxidations of olefinic alcohols by tert-butyl hydroperoxide. *J. Am. Chem. Soc.* **1973,** *95*, 6136.
61. Jeffrey, G.A. *An Introduction to Hydrogen Bonding*; Oxford University Press: New York, **1997**.
62. A similar intramolecular H-bond involving a vinyl epoxide O-atom was also observed in amphidinolide H in solid state as well as in solution. It is worth noting that the vinyl epoxide moiety of amphidinolide H serves as the actual trap for incoming biological nucleophiles. See: (a) Kobayashi, J.; Shimbo, K.; Sato, M.; Shiro, M.; Tsuda, M. Absolute Stereochemistry of Amphidinolides G and H. *Org. Lett.* **2000,** *2*, 2805; (b) Fürstner, A.; Bouchez, L. C.; Morency, L.; Funel, J.-A.; Liepins, V.; Poree, F.-H.; Gilmour, R.; Laurich, D.; Beaufils, F.; Tamiya, M. Total Syntheses of Amphidinolides B1, B4, G1, H1 and Structure Revision of Amphidinolide H2. *Chem. Eur. J.* **2009,** *15*, 3983.

Table of Contents